2009 American Control Conference
Hyatt Regency Riverfront, St. Louis, MO, USA
June 10-12, 2009

Control-Oriented Analysis of Thermal Gradients for a Hypersonic Vehicle

Sanketh Bhat and Rick Lind
University of Florida

Abstract— **Structural damage resulting from the tremondous heating incurred during hypersonic flight is mitigated by a thermal protection system; however, such mitigation is accompanied by an increase in weight that can be prohibitive. The actual design of a thermal protection system can be chosen to vary the level of heating reduction, and associated weight, across the structure. This paper considers how such designs and resulting thermal gradients influence the ability to achieve closed-loop performance. A control architecture is used that damps any thermal effects for a range of temperature profiles. Various designs are considered for a representative model to show the large variation in flight dynamics. The resulting closed-loop performance is characterized as a function of the induced thermal gradients to indicate the optimality of the designs.**

I. Introduction

Hypersonic flight is being agressively pursued as a capability to traverse the world in a few hours. A class of vehicles under consideration utilize a design in which a wedge-shaped fuselage provides lift and acts as an inlet for the SCRAMjet engine. This configuration and its associated aeropropulsive characteristics was successfully demonstrated on the X-43 prototype.

The design of hypersonic vehicles is maturing with respect to the aeropropulsive interactions of the fuselage and engine; however, the aerothermoelastic characteristics must also be addressed. Vibration attenuation is a critical requirement for these vehicles because any displacement of the fuselage will affect the engine performance. The control challenge is compounded by temperature effects that signficantly alter the structural dynamics throughout the flight as the fuselage heats.

A general model of the aeropropulsive dynamics has been developed based on a baseline vehicle [1] and extended to increase the fidelity [2], [3], [4] along with improving the structural dynamics [5], [6] and aerodynamics [7]. Using this model as a fixed design, several approaches for control have been considered including H_∞[8], μ synthesis[9] and Linear Parameter Varying(LPV) control[10]. Additional work has even considered sensor placement [11], [12].

Investigations into aerothermoelastic design are not as mature because of the challenges associated with simultaneous optimization of both the structure and the controller. Many previous efforts into the general problem of structure-control design have noted its inherent nonlinearities that can be solved using a variety of formulations including linear matrix inequalities and bi-linear matrix inequalities [13], [14], [15], [16].

Graduate Student, sanketh@ufl.edu
Associate Professor, ricklind@ufl.edu

This paper introduces a control-oriented analysis for hypersonic vehicles that directly considers mission capability. In this case, the analysis evaluates designs that seek to choose a thermal protection system and associated controller that maximize vibration attenuation.

The control-oriented analysis considers a parametrized solution to a Riccati equation. System design is intractable when trying to optimize both open-loop dynamics and feedback compensator simultaneously; alternatively, system design is actually manageable when trying to optimize the open-loop dynamics with respect to a feasibility condition that guarantees the existence of a feedback compensator. In this way, the actual controller does not need to be computed but merely an open-loop design for which a controller is guaranteed to exist will be designed.

This analysis technique initializes a concept of control-oriented design which represents a significant advancement to the state-of-the-art for the community and is particularly advantangeous for next-generation vehicles. Traditional approaches, which are satisfactory for traditional vehicles, will not be able to maximize mission capability for future classes of vehicles that will operate at off-cruise conditions, utilize high agility, include time-varying dynamics, and require complex interactions among the dynamics.

II. Closed-Loop Design Space

Systems are evaluated on their ability to perform missions; consequently, the design space must include all parameters that affect such ability. The closed-loop operation of such systems suggests a decomposition of the design space into separate subspaces. This decomposition follows the generalized block diagram, given in Figure 1, as a feedback relationship between the open-loop plant and a controller.

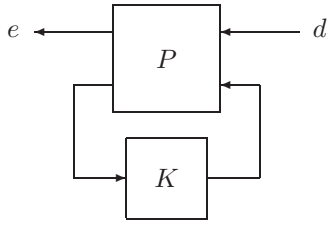

Fig. 1. Closed-Loop Block Diagram

A design space is formulated using the parameters that affect the open-loop dynamics. This space, defined as $\mathbb{P}$, can include a wide variety of parameters including geometry, structure, materials and other aspects related to vehicle

design. A particular configuration of the open-loop dynamics is thus represented by the vector, $\pi \in \mathbb{P}$, within the design space.

Another design space is formulated that contains the compensator elements that may be varied. This space, defined as $\mathbb{K}$, can include aspects of the feedback compensator such as gains, lags, bandwidth, and adaption rates along with sensors and actuators. Any controller is thus formulated using the vector, $\kappa \in \mathbb{K}$, from within the design space.

The set of closed-loop systems that are possible candidates for the optimal configuration can be represented by $\mathcal{T}$. This set notes that the open-loop plant, $P(\pi)$, depends on the design space of $\mathbb{P}$ and the compensator, $K(\kappa)$, depends on the design space of $\mathbb{K}$. Finally, the set of all closed-loop systems can be described as $\mathcal{T}$.

$$\mathcal{T} = \{F_l\left(P(\pi), K(\kappa)\right) \;\; \pi \in \mathbb{P}, \kappa \in \mathbb{K}\}$$

Also, the set of $\mathcal{T}$ can utilize a standard reduced-order model of the open-loop dynamics. Standard tools can compute state-space models using high-fidelty approaches from computational fluid dynamics or computational structural dynamics. A basic representation of a state-space model, $P = \{A, B, C, D\}$, is introduced although other representations can easily be substituted into the approach.

$$\mathcal{T} = \{F_l\left(\{A(\pi), B(\pi), C, D\}, K(\kappa)\right) \;\; \pi \in \mathbb{P}, \kappa \in \mathbb{K}\}$$

III. Feasibility-Based Optimization

The metric for design can be cast as an $\mathcal{H}_\infty$-norm condition on the closed-loop system. As such, the design seeks to find the optimal values for both the open-loop dynamics and an $\mathcal{H}_\infty$-norm controller. The computation for that controller is actually somewhat mature using a state-space solution although the joint computation of both dynamics and controller is intractable.

The optimal design actually does not need to compute both the open-loop dynamics and controller simultaneously; instead, the design can simply find the open-loop dynamics for which a controller exists that achieves the lowest $\mathcal{H}_\infty$-norm value.

The synthesis of controllers using modern techniques actually follows a two-step procedure. The initial step iterates over a feasibility check that indicates if a controller exists to achieve a particular value of closed-loop performance. The final step computes the gain for the feedback compensator that achieves the optimal closed-loop performance. This two-step procedure is implemented in professional software such as MATLAB, because a set of feasibility conditions is significantly less computationally expensive than a set of synthesis conditions.

The approach for control-oriented design is now expressed as minimizing the closed-loop norm with respect to the design space while maintaining the feasibility constraints.

$$\begin{gathered} \min \qquad \gamma \\ \pi \in \mathbb{P} \\ X = X^* > 0 \\ Y = Y^* > 0 \end{gathered}$$

subject to

$$\begin{aligned} 0 &= XA(\pi) + A(\pi)^* X \\ &\quad + X(\frac{1}{\gamma^2} B_1(\pi) B_1(\pi)^* - B_2(\pi) B_2(\pi)^*) X \\ &\quad + C_1(\pi) * C_1(\pi) \\ 0 &= A(\pi) Y + Y_A(\pi)^* \\ &\quad + Y(\frac{1}{\gamma^2} C_1(\pi)^* C_1(\pi) - C_2(\pi)^* C_2(\pi)) Y \\ &\quad + B_1(\pi) B_1(\pi)^* \\ \gamma^2 &> \rho(XY) \end{aligned}$$

This constrained optimization requires finding a minimum to a nonlinear function. The operators of X and Y, if they exist, can be found for any fixed value of π using standard algorithms; however, they are almost certain to have non-convex dependencies when considering all $\pi \in \mathbb{P}$. A variety of numerical approaches can be applied to the minimization including branch and bound, simulated annealing, neural networks, and so on.

Finally, the actual controller that achieves the optimal closed-loop system is computed using the solutions, X and Y, to these Riccati equations. The standard synthesis for $\mathcal{H}_\infty$-norm control is used.

IV. Example

A. Objective

A control-oriented design is optimized for a hypersonic vehicle. The mission objective is simply a prescribed change to airspeed and altitude; however, several difficulties must be circumvented for this basic maneuver. The propulsion system is tightly coupled to the fuselage so structural vibrations can cause loss of engine performance. The vibrations are compounded by the introduction of thermal gradients which result from the tremendous heating across the fuselage throughout flight. As such, vibration attenuation becomes a critical aspect of mission performance.

This example represents a single element within a larger multi-loop architecture [17]. The fundamental concept uses a pair of loops such that the inner-loop controller provides vibration attenuation while the outer-loop controller provides maneuvering. Such a loop decomposition recognizes that thermal effects are predominantly limited to the structural dynamics related to vibration. The outer-loop controller is thus designed without consideration of temperature effects since the inner-loop controller is assumed to provide adequate compensation.

A baseline vehicle is adopted from an extensive program by the U.S. Air Force for a reduced-order model [2], [3], [4], [5], [6], [7]. This model includes 5 states for the rigid-body flight dynamics and an additional 6 states associated with 3 flexible-body structural dynamics. The model is particularly attractive in that it contains a rigorous derivation of the aerothermoelastic coupling that explicitly highlights the effects of vibrations on mission performance.

B. Design Space

The design space for the open-loop dynamics consists of a 2-dimensional set, $\mathbb{P}$, related to effective temperature. In this case, a set of thermal profiles are chosen that have constant gradient from the nose to tail. This set, as shown in Figure 2, considers variations in both the tail temperature and nose temperature.

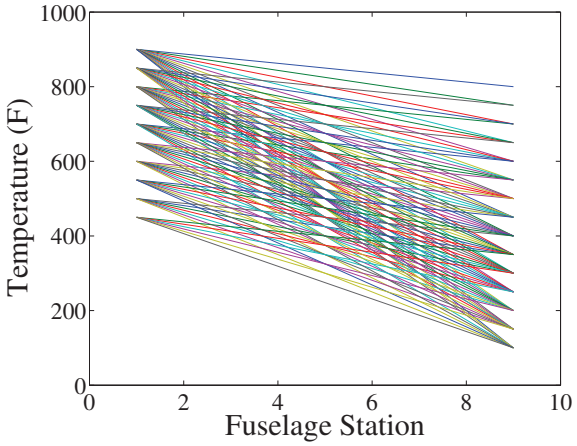

Fig. 2. Thermal Profiles Comprising the Design Space

The open-loop dynamics are parametrized as function of these effective temperatures to reflect variations in the Young's modulus at the nose and tail which result from the structural elements and thermal protection system. A set of variables that are representative of the parametrization around the design space are noted in Figure 3 for the influence of bending-mode displacement on the velocity and in Figure 4 for the influence of elevator on the bending-mode velocity.

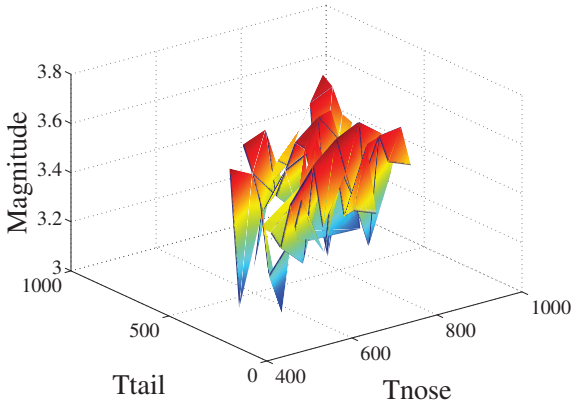

Fig. 3. Open-Loop Stability Coefficient as a Function of Design Space

C. Control Synthesis

A synthesis model is formulated that relates the open-loop dynamics to a set of errors and disturbances. These errors are specifically chosen such that their size is directly inverse to the closed-loop performance for vibration attenuation. This model is shown in Figure 5 as a block diagram.

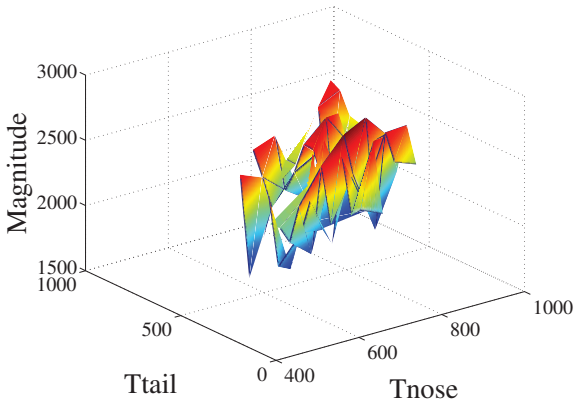

Fig. 4. Open-Loop Control Coefficient as a Function of Design Space

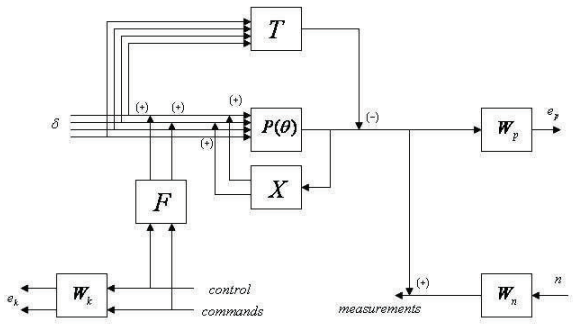

Fig. 5. Synthesis Model

A model-matching approach is chosen to specify a desired level of vibration attenuation. As such, a target model is given as T in the synthesis model that represents dynamics with appropriate damping on the structural mode. The transfer functions are shown in Figure 6 for both the nominal open-loop dynamics and the target dynamics. Note the peak near 0.04 *rad/s* is associated with a rigid-body flight mode while the peak near 22 *rad/s* is associated with the structural mode that should be attenuated.

A feedback compensator is given as X in the synthesis model. This compensator is only included to stabilize the open-loop dynamics. Essentially, the controller is being designed to only augment damping of the structural mode without introducing any variations to the low-frequency behavior. The $\mathcal{H}_\infty$-norm synthesis is required to stabilize the closed-loop system so X is included to ensure the resulting controller does not affect the rigid-body modes through stabilization. The final multi-loop architecture will introduce an outer-loop controller to replace X and provide both stability and performance for the rigid-body maneuvering.

An error signal, $e_p \in \mathcal{R}$, is defined to represent the tracking performance. This signal is a weighted difference between the actual pitch rate and the desired pitch rate. The

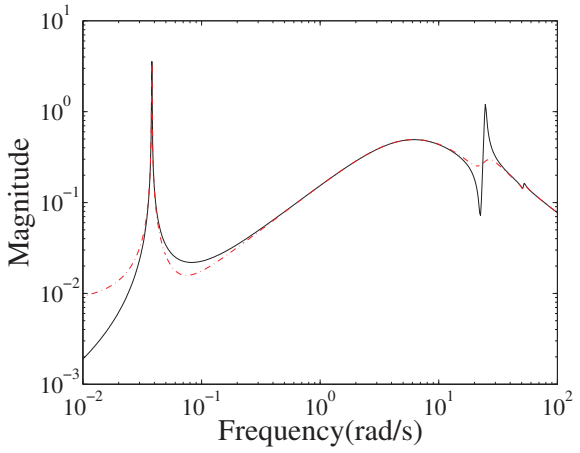

Fig. 6. Nominal Model (—) and Target Model (– – –)

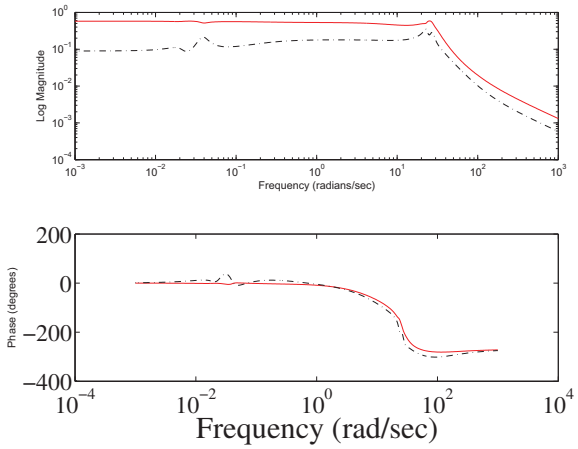

Fig. 7. Optimal Controller from Pitch Rate to Elevator (—) and Canard (– – –)

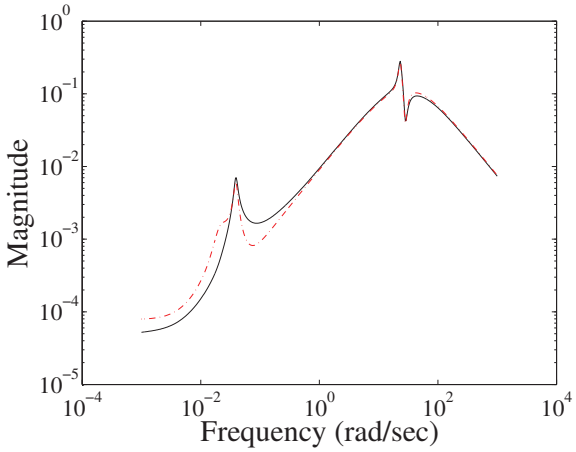

Fig. 8. Actual (—) and Desired (– – –) Transfer Function

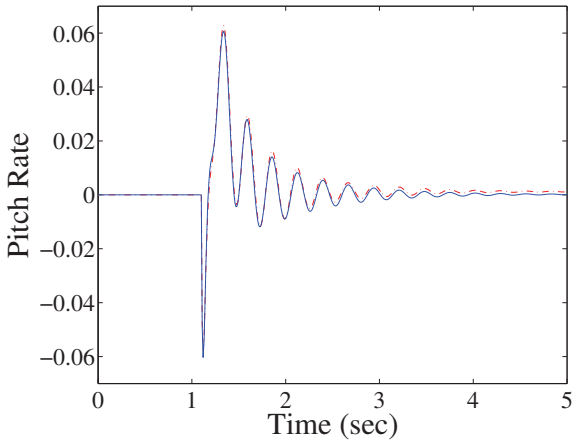

Fig. 9. Actual (—) and Desired (– – –) Closed-Loop Response

weighting, $W_P = \frac{s+100}{s+5}$, is chosen to reflect the frequency range over which tracking is desired.

An error signal, $e_K \in \mathcal{R}^2$, is defined to represent the actuation penalty on elevator and canard. This signal is generated by weighting the command to each surface through $W_k = \frac{s+10}{s+100}$ to reflect a larger penalty on high-frequency actuation.

Noise, n, is associated with the sensor measurement of pitch rate. This signal is weighted through $W_n = 0.01$ to limit the relative size of this noise in comparison to the pitch rate.

D. Control-Oriented Design

A control-oriented design is performed to choose the structure and thermal protection system along with the controller. In this case, an $\mathcal{H}_\infty$-norm synthesis is used that considers the pair of parametrized Riccati equations. A basic algorithm for constrained optimization generates a design that corresponds to a local minimum of the cost function.

The optimal elements of the design space are chosen as $\pi = [750, 450]$ and the controller, κ, whose Bode plot is shown in Figure 7. As such, the value of π indicates the lowest closed-loop norm is achieved if the thermal protection system is chosen to have a nose temperature of 750^o and a tail temperature of 450^o.

The transfer function of the closed-loop system is shown in Figure 8 as similar to the target model. The relationship between pitch rate and elevator are close at all frequencies but particularly close near the natural frequency of the bending mode. As such, the objective of high-frequency vibration attenuation without altering the low-frequency dynamics is essentially achieved.

The resulting vibration attenuation and associated actuation is shown in Figure 9.

The optimality of the system can be verified by comparing the performance metrics for the control-oriented design to a complete design over system in the design space. This comparison is relatively easy to do for this system; however, it would be prohibitive to compute closed-loop designs for each configuration with a high-dimensional design space. In this case, the control-oriented design was able to achieve a closed-loop norm of 0.22.

E. Analysis

The relationship between the design space and the closed-loop performance can be explored. In particular, the complexity between open-loop design and closed-loop design should be evaluated to determine the additional cost induced

by the addition of control synthesis to the procedure.

The difficulty of optimizing an open-loop design are understood. Certainly the open-loop dynamics, as evidenced in Figure 3, have a highly nonlinear parameterization around the design space. A functional based on this nonlinear parametrization would thus have to be minimized to obtain optimality in any open-loop design.

The closed-loop norm can similarly be parametrized around the design space. In this case, a set of controllers are generated for each thermal profile in Figure 2 and associated open-loop plant in Figure 3. The resulting closed-loop norm, as shown in Figure 10, shows a remarkably similar parametrization as the open-loop dynamics.

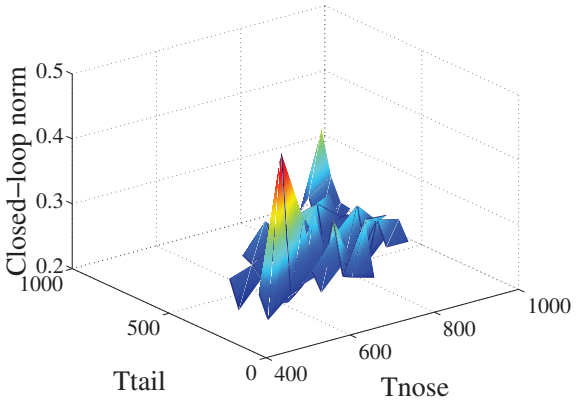

Fig. 10. Closed-Loop Norm Parametrized around Design Space

The reason for the similarity between parameterizations of open-loop dynamics and closed-loop dynamics is found by investigating a different relationship; namely, the closed-loop norm should be parameterized as a function of the open-loop dynamics instead of the design space. The closed-loop norm and associated performance for tracking is actually directly related to the parameters of the open-loop state-space model. This result is certainly expected; however, the independence of that relationship from temperature as shown in Figure 11 is not completely anticipated.

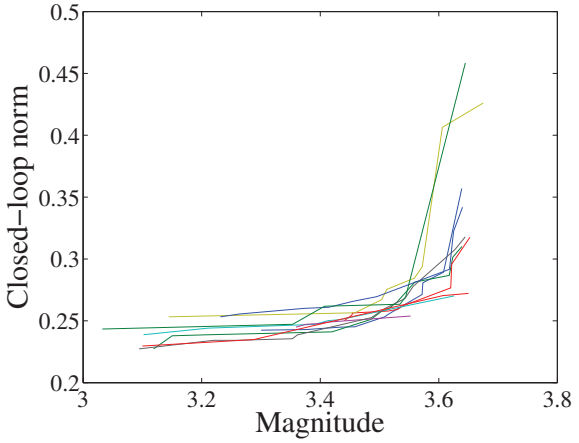

Fig. 11. Closed-Loop Norm Parametrized around Open-Loop Dynamics

A control-oriented design is thus demonstrated to be similar in difficulty to open-loop design. The introduction of control synthesis merely adds a linear dependency onto a nonlinear dependency which does not overly increase the computational challenge.

F. Sensitivity

Also, the sensitivity of the design to nonlinear dependencies should be noted. The dynamics, as shown in Figure 3, are strongly nonlinear across the design space so the optimization is almost certain to reach only a local minimum. Such local minima are not necessarily accompanied by poor performance since several such local minima have closed-loop norms within 5% of the global minimum. The data in Figure 12 shows that several thermal profiles associated with local minima and the resulting performance in Figure 13 can compare favorably with the global minima and its resulting performance.

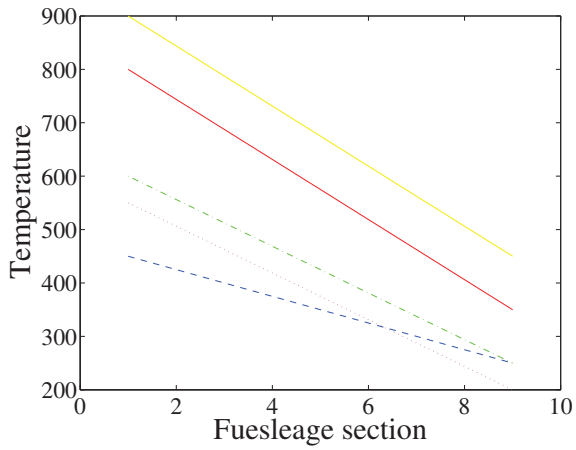

Fig. 12. Thermal Profiles Associated with Similarly-Valued Local Minima

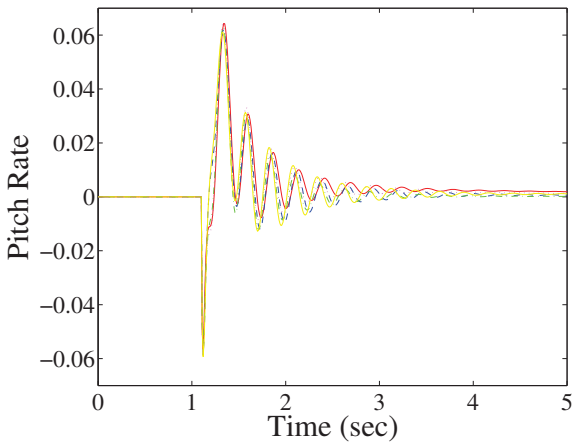

Fig. 13. Closed-Loop Performance for each Thermal Profile

This sensitivity presents an interesting feature of the hypersonic vehicle; namely, similar levels of closed-loop performance can be achieved for several choices of thermal profiles if they are designed properly. The profiles shown in Figure 12 allow for similar closed-loop performance so the associated thermal protection systems can be further evaluated for issues such as weight and cost to optimize the design for additional metrics.

V. Conclusion

Vibration attenuation is a critical requirement for maintaining hypersonic flight for a coupled fuselage-engine configuration. Such attenuation can be facilitated by designing both a thermal protection system and feedback controller that can compensate for the variations in the structural dynamics due to temperature profile. This paper has introduced a control-oriented design by which the open-loop system is designed to achieve the maximum level of performance for which a controller exists. A representative model of a hypersonic vehicle is used to demonstrate this approach can indeed generate a design.

VI. Acknowledgements

This work was supported through NASA NNX07AC46A with Donald Soloway as program manager.

References

[1] F. Chavez and D. Schmidt, "Analytical Aeropropulsive/Aeroelastic Hypersonic-Vehicle Model with Dynamic Analysis," *Journal of Guidance, Control and Dynamics*, Vol. 17, No. 6, Nov-Dec 1994, pp. 1308-1319.

[2] M. Bolender and D. Doman, "A Non-linear Model for the Longitudinal Dynamics of a Hypersonic Air-Breathing Vehicle," *AIAA Guidance, Navigation and Control Conference*, 2005, AIAA-2005-6255.

[3] M. Bolender and D. Doman, "Nonlinear Longitudinal Dynamical Model of an Air-Breathing Hypersonic Vehicle," *Journal of Spacecraft and Rockets*, Vol. 44, No. 2, March-April 2007, pp. 374-387.

[4] M. Bolender and D. Doman, "Modeling Unsteady Heating Effects on the Strucutral Dynamics of a Hypersonic Vehicle," *AIAA Atmospheric Flight Mechanics Conference*, 2006, AIAA-2006-6646.

[5] T. Williams, M. Bolender, D. Doman and O. Morataya, "An Aerothermal Flexible Model Analysis of a Hypersonic Vehicle," *AIAA Atmospheric Flight Mechanics Conference*, 2006, AIAA-2006-6647.

[6] A. Culler, T. Williams and M. Bolender, "Aerothermal Modeling and Dynamic Analysis of a Hypersonic Vehicle," *AIAA Atmospheric Flight Mechanics Conference*, 2007.

[7] M. Oppenheimer, T. Skijins, M. Bolender and D. Doman, "A Flexible Hypersonic Vehicle Model Developed With Piston Theory," *AIAA Atmospheric Flight Mechanics Conference*, 2007, AIAA-2007-6396.

[8] H. Buschek and A. Calise, "Fixed Order Robust Control Design for Hypersonic Vehicles," *AIAA Guidance, Naviagation and Control Conference*, AIAA-94-3662,1994.

[9] H. Buschek and A. Calise, "Robust Control of Hypersonic Vehicles Considering Propulsive and Aeroelastic Effects," *AIAA Guidance, Navigation and Control Conference*, AIAA-93-3762,1993.

[10] R. Lind, "Linear Parameter-Varying Modeling and Control of Structural Dynamics with Aeroelastic Effects,"*Journal of Guidance, Control and Dynamics*, Vol. 25, No. 4,2001, pp. 733-739.

[11] P. Jankovsky, D. Sigthorsson, A. Serrani, S. Yurkovich, M. Bolender and D. Doman, "Output Feedback Control and Sensor Placement for a Hypersonic Vehicle Model," *AIAA Guidance,Navigation, and Control Conference*, 2007, AIAA-2007-6327.

[12] L. Fiorentini, A. Serrani, M. Bolender and D. Doman, "Nonlinear Robust/Adaptive Controller Design for an Air-Breathing Hypersonic Vehicle Model," *AIAA Guidance,Navigation and Control Conference*, 2007, AIAA-2007-6329.

[13] M.G. Safonov, K.C. Goh and J.H. Ly, "Control System Synthesis via Bilinear Matrix Inequalities," *IEEE American Control Conference*, 1994, pp. 45-49.

[14] G. Shi and R.E. Skelton, "An Algorithm for Integrated Structure and Control Design with Variance Bounds," *IEEE Conference on Decision and Control*, 1996, pp. 167-172.

[15] T. Tanaka and T. Sugie, "General Framework and BMI Formulae for Simultaneous Design of Structure and Control Systems," *IEEE Conference on Decision and Control*, 1997, pp. 773-778.

[16] H.D. Tuan and P. Apkarian, "Low Nonconvexity-Rank Bilinear Matrix Inequalities: Algorithms and Applications in Robust Controller and Structure Design," *IEEE Transactions on Automatic Control*, Vol. 45, No. 11, November 2000, pp. 2111-2117.

[17] R. Lind, J.L. Buffington, and A.K. Sparks, "Multi-Loop Aeroservoelastic Control of a Hypersonic Vehicle," *AIAA Guidance, Navigation, and Control Conference*, 1999, AIAA-99-4123.